J. Fluid Mech. (1982), *vol.* 120, *pp.* 71–89
Printed in Great Britain

Non-uniform discharges of contaminants in shear flows

By RONALD SMITH

Department of Applied Mathematics and Theoretical Physics,
University of Cambridge, Silver Street, Cambridge CB3 9EW

(Received 14 September 1981 and in revised form 27 January 1982)

For a non-uniform discharge of contaminant in a shear flow the initial advection velocity and the amount of shear across the contaminant cloud depend upon the discharge shape across the flow. Here it is shown how the continuing influence of the discharge non-uniformity can be incorporated into a delay-diffusion description of the dispersion process (Smith 1981). An important improvement over the variable coefficient diffusion equation derived by Gill & Sankarasubramanian (1971) is that the solutions have the physically correct superposition property.

1. Introduction

In studies of contaminant dispersion in laterally confined flows it often suffices to know bulk quantities such as the cross-sectionally averaged concentration $\bar{c}(x,t)$. Thus much theoretical effort has been directed towards the development of appropriate bulk-model equations. It is now well established that, at large times after discharge, the evolution of $\bar{c}(x,t)$ is accurately described by a constant-coefficient diffusion equation (Taylor 1953). Unfortunately, the large-time restriction is quite stringent (Chatwin 1970). An attractive way around this difficulty is to permit the coefficients to be time-dependent. For a sudden uniform discharge at $t = 0$, Gill & Sankarasubramanian (1970) derived the longitudinal dispersion equation

$$\partial_t \bar{c} + \bar{u}\,\partial_x \bar{c} - [\bar{\kappa} + D(t)]\,\partial_x^2 \bar{c} = 0. \tag{1.1}$$

Here $\bar{u}$ is the bulk velocity, $\bar{\kappa}$ the cross-sectionally averaged longitudinal diffusivity, and $D(t)$ the time-dependent shear-dispersion coefficient. This model equation has the remarkable properties that the area, centroid and variance are all exact.

For a non-uniform discharge, the initial advection velocity and rate of shear distortion of the contaminant distribution depend strongly upon whereabouts across the flow the discharge was made (see figure 1). Gill & Sankarasubramanian (1971) showed that this additional complication could be dealt with by means of the extended equation

$$\partial_t \bar{c} + [\bar{u} + \partial_t \hat{X}]\,\partial_x \bar{c} - [\kappa + D(t) + \hat{D}(t) - \hat{X}\,\partial_t \hat{X}]\,\partial_x^2 \bar{c}. \tag{1.2}$$

Here $\hat{X}(t)$ is the centroid displacement and $\hat{D}(t)$ the excess shear dispersion associated with the non-uniformity of the discharge. Again, the area, centroid and variance are all exact.

A mathematically convenient feature of (1.1), (1.2) is that they admit of exact analytic solutions. For example, the solution for a point discharge is exactly Gaussian:

$$\bar{c} = \exp(-\tfrac{1}{2}[x - \hat{X} - \bar{u}t]^2/\sigma^2)/\sigma(2\pi)^{\frac{1}{2}},$$

with

$$\sigma^2 = 2\bar{\kappa}t + 2\int_0^t [D + \hat{D}]\,dt' - \hat{X}^2. \tag{1.3}$$

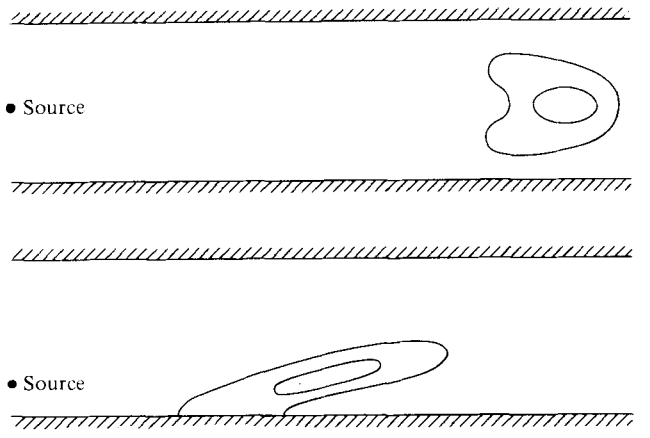

FIGURE 1. Sketch of contaminant clouds at the same time after discharge for two different source positions across a flow.

Unfortunately, when it comes to physical interpretation, (1.2) has serious shortcomings. As has been emphasized by Taylor (1959), a basic requirement for any model of contaminant dispersion is that the solutions can be superimposed. Equation (1.2) does not have this property. For example, if there are independent point discharges involving two different non-uniformities then the concentration distribution in both cases is Gaussian with standard deviations

$$\left.\begin{aligned}\sigma_1^2 &= 2\bar{\kappa}t + 2\int_0^t [D+\hat{D}_1]\,dt' - \hat{X}_1^2,\\ \sigma_2^2 &= 2\bar{\kappa}t + 2\int_0^t [D+\hat{D}_2]\,dt' - \hat{X}_2^2.\end{aligned}\right\} \tag{1.4}$$

The superposition of the two different Gaussian profiles is not Gaussian. However, if we were to apply (1.2) to a composite discharge with strengths ξ_1, ξ_2 then we would have

$$\hat{X} = \frac{\xi_1\hat{X}_1 + \xi_2\hat{X}_2}{\xi_1+\xi_2}, \quad \hat{D} = \frac{\xi_1\hat{D}_1 + \xi_2\hat{D}_2}{\xi_1+\xi_2}, \tag{1.5}$$

and the solution (1.3) would again be exactly Gaussian. Thus the superposition property is violated. Similarly, if there are discharges at diverse times then $\hat{X}$, $\hat{D}$ are multivalued and the composite contaminant distribution does not satisfy an equation of the form (1.2).

Aware of such fundamental shortcomings of Gill & Sankarasubramanian's model equation (1.2), Maron (1978) proposed a rational alternative

$$\partial_t\bar{c} + \bar{u}\,\partial_x\bar{c} - \bar{\kappa}\,\partial_x^2\bar{c} - \int_0^\infty \partial_\tau D\,\partial_x^2\bar{c}(x-\bar{u}\tau, t-\tau)\,d\tau = \bar{q} - \sum_{m=1}^{\infty}\int_0^\infty \partial_\tau X_m\,\partial_x q_m(x-\bar{u}\tau, t-\tau)\,d\tau. \tag{1.6}$$

Here $q_m(x,t)$ is the strength of the mth-mode non-uniformity and $X_m(\tau)$ is the corresponding centroid displacement. Linear superposition is ensured by the fact that the right-hand side $\bar{q}$ and q_m terms do not involve $\bar{c}$. Also, discharges at different times are permitted. The rate of dispersion associated with earlier discharges is relatively large because the $\partial_\tau D$ integral extends further back in time.

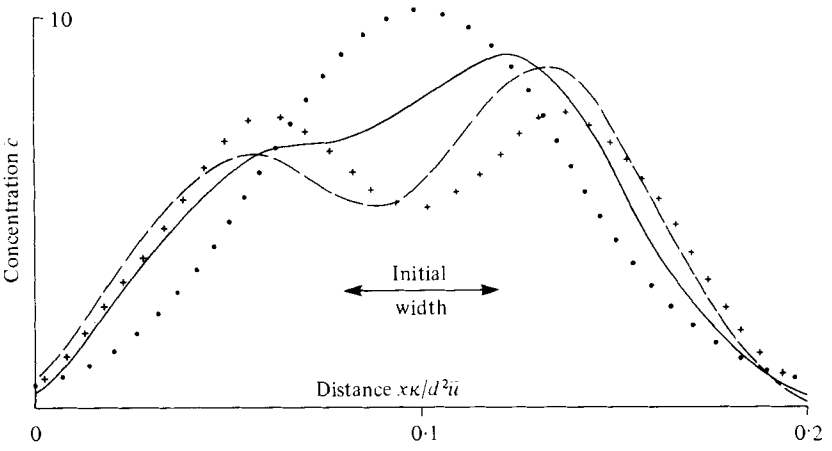

FIGURE 2. Comparison between the exact numerical results of Jayaraj & Subramanian (1978) (——), the diffusion solution of Krishnamurthy & Subramanian (1977) (· · · · ·), the solution of Maron's equation (1·6) (+ + + +), and the solution of the delay-diffusion equation (1·8) (– – – –) for plane Poiseuille flow at time $0{\cdot}1d^2/\kappa$ after discharge.

Maron (1978) alludes to inadequacies of the predicted concentration profiles, but he does not give any examples. Presumably, this is because unlike (1.1), (1.2) Maron's equation (1.6) does not admit of analytic solutions, and is solvable only by numerical techniques. Figure 2 reveals that the distinctive feature is the existence of exaggerated and incorrectly positioned concentration peaks to the front and to the rear of the concentration distribution. Thus, there would seem to be a choice between a reasonably accurate but philosophically unsound model equation (1.2) and a philosophically sound but less accurate model (1.6).

Fortunately, if the memory displacement $\bar{u}\tau$ on the left-hand side of (1.6) is replaced by

$$\int_0^\tau v_0(\tau')\,d\tau' \tag{1.7}$$

(Smith 1981), then for uniform discharges the delay-diffusion equation (1.6) can yield more accurate concentration predictions than the rival equation (1.1). The exaggerated peakiness remains. However, the asymmetry of the heights of the peaks is in reasonable agreement with the exact results (see figure 2). Maron's equation and the diffusion equation share the shortcoming that for symmetric discharges they yield symmetric solutions. By contrast, with the optimal choice of $v_0(\tau)$, not only are the area, centroid and variance exact, but also the delay-diffusion equation yields the exact skewness (Smith 1981, § 4).

In the present paper we are concerned to improve the modelling of non-uniform discharges. The resulting modified version of (1.6) is

$$\partial_t\bar{c}+\bar{u}\,\partial_x\bar{c}-\bar{\kappa}\,\partial_x^2\bar{c}-\int_0^\infty \partial_\tau D\,\partial_x^2\bar{c}\left(x-\int_0^\tau v_0(\tau')\,d\tau',t-\tau\right)d\tau$$
$$=\bar{q}-\sum_{m=1}^{\infty}\int_0^\infty \partial\hat{\tau}\,X_m\,\partial_x q_m\left(x-\int_0^\tau v_m(\tau')\,d\tau',t-\tau\right)d\tau. \tag{1.8}$$

Thus there is a different memory velocity $v_m(\tau)$ for each mode. The crucial feature inherited in Maron's equation (1.6) is that the solutions have the physically correct

linear superposition property with respect to both varied discharge times and different discharge positions across the flow.

Although (1.8) does not admit of analytic solutions, it is shown in § 6 how suitable (two-layer) approximations for $\partial_\tau D$, $\partial_\tau X_m$ and v_m lead to a telegraph equation for which explicit solutions are known (Thacker 1976). Moreover, these (two-layer) solutions accurately reproduce the marked skewness of the full solution $\bar{c}(x,t)$ at moderately large times after discharge (Chatwin 1970).

2. Representation of the concentration variations

In keeping with the generality of the dispersion concept, we present the analysis for flow in a region of arbitrary cross-sectional shape, and with a diffusivity which may vary across the flow:

$$\partial_t c + u\,\partial_x c - \kappa \partial_x^2 c - \nabla . (\kappa \nabla c) = q, \tag{2.1}$$

with

$$\kappa \mathbf{n} . \nabla c = 0 \quad \text{on } \partial A.$$

Here x is the longitudinal co-ordinate, (y,z) the cross-stream co-ordinates, ∇ the two-dimensional gradient operator $(0, \partial_y, \partial_z)$, $c(x,y,z,t)$ the concentration, $u(y,z)$ the longitudinal velocity, $q(x,y,z,t)$ the source distribution, $\kappa(y,z)$ the diffusivity, A the flow region, ∂A its boundary, and $\mathbf{n}$ the outward normal.

The linearity of (2.1) means that we can superimpose solutions corresponding to different source distributions. This leads us to introduce a complete set of functions $\{\phi_m(y,z)\}$ such that the departure from uniformity can be written

$$q(x,y,z,t) - \bar{q}(x,t) = \sum_{m=1}^{\infty} q_m(x,t)\,(\phi_m(y,z) - \overline{\phi}_m). \tag{2.2}$$

In §§ 4, 5 we find that the ideal choice for the basis functions are the normal modes $\{\psi_m\}$ for the free decay of concentration variations across the flow. A crucial feature is that it is the coefficients $q_m(x,t)$ and not the functions $\phi_m(y,z)$ that depend upon the discharge shape, as otherwise it is difficult to preserve the superposition property in any approximation scheme.

Within the confines of a bulk model we cannot expect to solve (2.1) exactly. However, instead of stating a once-and-for-all approximation, we follow Gill & Sankarasubramanian (1970, 1971) and embed our intuitive guess in a formal series expansion. For a non-uniform discharge with a single-mode structure $q_m(x,t)\,\phi_m(y,z)$, we pose the series solution

$$c = \bar{c} + \sum_{j=1}^{\infty} \int_0^{\infty} l_j(y,z,\tau)\,\partial_x^j \bar{c}\left(x - \int_0^{\tau} v_0(\tau')\,d\tau', t-\tau\right) d\tau$$
$$+ \sum_{j=0}^{\infty} \int_0^{\infty} f_{mj}(y,z,\tau)\,\partial_x^j q_m \left(x - \int_0^{\tau} v_m(\tau')\,d\tau', t-\tau\right) d\tau. \tag{2.3}$$

Physically, the integral terms represent the way in which concentration gradients across the flow are generated at earlier times by the shear rotation of longitudinal gradients, and are then advected downstream. The $\partial_x^j \bar{c}$ terms are precisely as obtained by Smith (1981), and the $\partial_x^j q_m$ terms allow for the fading memory of the non-uniform concentration discharge. Thus the concern of the present paper is to determine the

new f_{mj} coefficients and the displacement velocities v_m. For a general discharge there would be a summation with respect to m in order to account for the full non-uniformity (2.2).

3. Longitudinal and transverse dispersion equations

If the ansatz (2.3) is substituted into the cross-sectionally averaged diffusion equation (2.1), then we arrive at the integro-differential equation

$$\begin{aligned}&\partial_t \bar{c} + \bar{u}\,\partial_x \bar{c} - \bar{\kappa}\,\partial_x^2 \bar{c} \\ &\quad - \sum_{j=2}^{\infty} \int_0^{\infty} [\overline{(\kappa-\bar{\kappa}) l_{j-2}} + \overline{(\bar{u}-u) l_{j-1}}]\, \partial_x^j \bar{c} \left(x - \int_0^{\tau} v_0(\tau')\, d\tau', t-\tau\right) d\tau \\ &\quad = \bar{q} + \sum_{j=1}^{\infty} \int_0^{\infty} [\overline{(\kappa-\bar{\kappa}) f_{mj-2}} + \overline{(\bar{u}-u) f_{mj-1}}]\, \partial_x^j q_m \left(x - \int_0^{\tau} v_m(\tau')\, d\tau', t-\tau\right) d\tau, \quad (3.1)\end{aligned}$$

where the overbars denote cross-sectional average values. The lowest-order truncation that includes the effects of shear dispersion and of discharge non-uniformity is the delay-diffusion equation (1.8) with

$$\partial_\tau D = \overline{(\bar{u}-u) l_1}, \quad \partial_\tau X_m = \overline{(u-\bar{u}) f_{m0}}. \quad (3.2)$$

Mathematically the complete longitudinal dispersion equation (3.1) enables us to write the time derivatives in terms of x-derivatives:

$$\begin{aligned}\partial_t c = \partial_t \bar{c} + \sum_{j=1}^{\infty} l_j(y,z,0)\, \partial_x^j \bar{c} + \sum_{j=1}^{\infty} \int_0^{\infty} (\partial_\tau l_j - v_0 l_{j-1})\, \partial_x^j \bar{c}\, d\tau \\ + \sum_{j=0}^{\infty} f_{mj}(y,z,0)\, \partial_x^j q_m + \sum_{j=0}^{\infty} \int_0^{\infty} (\partial_\tau f_m - v_m f_{m-1})\, \partial_x^j q_m d\tau, \quad (3.3)\end{aligned}$$

with $\partial_t \bar{c}$ given by (3.1). Thus it is now possible to write the three-dimensional dispersion equation (2.1) as a series:

$$\begin{aligned}&[l_1(y,z,0) + u - \bar{u}]\, \partial_x \bar{c} + [l_2(y,z,0) + \bar{\kappa} - \kappa]\, \partial_x^2 \bar{c} + \sum_{j=3}^{\infty} l_j(y,z,0)\, \partial_x^j \bar{c} \\ &\quad + [f_{m0}(y,z,0) + \bar{\phi}_m - \phi_m] q_m + \sum_{j=1}^{\infty} f_{mj}(y,z,0)\, \partial_x^j q_m \\ &\quad + \sum_{j=1}^{\infty} \int_0^{\infty} [\partial_\tau l_j - v_0(\tau) l_{j-1} + u l_{j-1} - \overline{u l_{j-1}} - \kappa l_{j-2} + \overline{\kappa l_{j-2}} - \nabla \cdot (\kappa \nabla l_j)] \\ &\quad \times \partial_x^j \bar{c} \left(x - \int_0^{\tau} v_0(\tau')\, d\tau', t-\tau\right) d\tau \\ &\quad + \sum_{j=0}^{\infty} \int_0^{\infty} [\partial_\tau f_{mj} - v_m(\tau) f_{mj-1} + u f_{mj-1} - \overline{u f_{mj-1}} - \kappa f_{mj-2} + \overline{\kappa f_{mj-2}} - \nabla \cdot (\kappa \nabla f_{mj})] \\ &\quad \times \partial_x^j q_m \left(x - \int_0^{\tau} v_m(\tau')\, d\tau', t-\tau\right) d\tau = 0,\end{aligned}$$

with

$$\begin{aligned}&\sum_{j=1}^{\infty} \int_0^{\infty} \kappa \mathbf{n} \cdot \nabla l_j\, \partial_x^j \bar{c} \left(x - \int_0^{\tau} v_0(\tau')\, d\tau', t-\tau\right) d\tau \\ &\quad + \sum_{j=0}^{\infty} \kappa \mathbf{n} \cdot \nabla f_{mj}\, \partial_x^j q_m \left(x - \int_0^{\tau} v_m(\tau')\, d\tau', t-\tau\right) d\tau = 0 \quad \text{on } \partial A. \quad (3.4)\end{aligned}$$

Proceeding as in Smith (1981), we argue that since the equations should be valid for arbitrary $\bar{c}$, q_m then the component equations corresponding to $\partial_x^j \bar{c}$, $\partial_x^j q_m$ should be satisfied separately. The resulting transverse dispersion equations for the f_{mj} functions are

$$\left.\begin{aligned} &\partial_\tau f_{m0} - \nabla.(\kappa \nabla f_{m0}) = 0, \\ \text{with} \quad &f_{m0} = \phi_m - \overline{\phi}_m \quad \text{at} \quad \tau = 0 \quad \text{and} \quad \kappa \mathbf{n}.\nabla f_{m0} = 0 \quad \text{on} \quad \partial A, \end{aligned}\right\} \tag{3.5}$$

$$\left.\begin{aligned} &\partial_\tau f_{m1} - \nabla.(\kappa \nabla f_{m1}) = \overline{u f_{m0}} - u f_{m0} + v_m(\tau) f_{m0}, \\ \text{with} \quad &f_{m1} = 0 \quad \text{at} \quad \tau = 0 \quad \text{and} \quad \kappa \mathbf{n}.\nabla f_{m1} = 0 \quad \text{on} \quad \partial A, \end{aligned}\right\} \tag{3.6}$$

$$\left.\begin{aligned} &\partial_\tau f_{mj} - \nabla.(\kappa \nabla f_{mj}) = \overline{u f_{mj-1}} - u f_{mj-1} + v_m(\tau) f_{mj} + \kappa f_{mj-2} - \overline{\kappa f_{mj-2}}, \\ \text{with} \quad &f_{mj} = 0 \quad \text{at} \quad \tau = 0 \quad \text{and} \quad \kappa \mathbf{n}.\nabla f_{mj} = 0 \quad \text{on} \quad \partial A. \end{aligned}\right\} \tag{3.7}$$

The equations for the l_j coefficients are precisely as derived by Smith (1981, equations (2.5)–(2.7)), and therefore have been omitted here.

4. Eigenfunction expansions

To solve the transverse dispersion equations (3.5)–(3.7), we follow Gill & Sankarasubramanian (1971) and introduce the eigenfunctions $\psi_j(y, z)$ for diffusion across the flow:

$$\left.\begin{aligned} &\nabla.(\kappa \nabla \psi_j) + \lambda_j \psi_j = 0, \\ \text{with} \quad &\kappa \mathbf{n}.\nabla \psi_j = 0 \quad \text{on} \quad \partial A. \end{aligned}\right\} \tag{4.1}$$

The ideal choice for the non-uniformity functions $\phi_m - \overline{\phi}_m$ is to take $\phi_m = \psi_m$. Otherwise, we need the connection formulae

$$\phi_m - \overline{\phi}_m = \sum_{j=1}^{\infty} \alpha_{mj} \psi_j(y, z) / (\overline{\psi_j^2})^{\frac{1}{2}}. \tag{4.2}$$

From (3.5) it follows that the corresponding representation for f_{m0} is given by

$$f_{m0} = \sum_{j=1}^{\infty} a_{mj} \exp(-\lambda_j \tau) \psi_j(y, z) / (\overline{\psi_j^2})^{\frac{1}{2}}. \tag{4.3}$$

Before we can use an eigenfunction expansion to solve (3.6), it is first necessary to determine a suitable representation for the right-hand-side forcing terms. To do this, we introduce the coefficients

$$u_{ln} = \overline{u \psi_l \psi_n} / (\overline{\psi_l^2})^{\frac{1}{2}} (\overline{\psi_n^2})^{\frac{1}{2}}. \tag{4.4}$$

The resulting expression for the forcing is

$$\overline{u f_{m0}} - u f_{m0} + v_m(\tau) f_{m0} = \sum_{n=1}^{\infty} [v_m(\tau) \alpha_{mn} \exp(-\lambda_n \tau) - \sum_{l=1}^{\infty} u_{ln} \alpha_{ml} \exp(-\lambda_l \tau)] \psi_n / (\overline{\psi_n^2})^{\frac{1}{2}}. \tag{4.5}$$

Solving (3.6) for each eigenmode separately, we can derive the composite solution

$$f_{m1} = \sum_{n=1}^{\infty} \alpha_{mn} \left[\int_0^\tau v_m(\tau') \, d\tau' - u_{nn} \tau \right] \exp(-\lambda_n \tau) \psi_n / (\overline{\psi_n^2})^{\frac{1}{2}} - \sum_{n=1}^{\infty} \sum_{l \neq n} \alpha_{ml} u_{ln} \left\{ \frac{\exp(-\lambda_n \tau) - \exp(-\lambda_l \tau)}{\lambda_l - \lambda_n} \right\} \psi_n / (\overline{\psi_n^2})^{\frac{1}{2}}. \tag{4.6}$$

Although we shall not pursue the detailed solutions for the higher-order coefficients, it is of interest to confirm that the lower-order terms are dominant. The argument used by Gill & Sankarasubramanian (1971, equation (44)–(56)) can readily be adapted to show that for small times

$$f_{mj} = O(\tau^j/j!) \quad \text{for} \quad \nabla\kappa = 0. \tag{4.7}$$

Thus it is the first few terms in the f_{mj} series that have the dominant contribution to $c-\bar{c}$. In the general case, with $\nabla\kappa$ non-zero, the initial growth rates are somewhat larger,

$$f_{m2j-1},\quad f_{m2j} = O(\tau^j/j!) \quad \text{for} \quad \nabla\kappa \neq 0, \tag{4.8}$$

but the conclusion remains valid. At large times after discharge the memory of the source distribution across the flow decays exponentially on a time scale of λ_1^{-1}. Thus the full f_{mj} series is negligible, and truncation at any level is justifiable.

5. Centroid and memory velocities

In terms of the eigenfunctions $\psi_j(y,z)$, the velocity profile $u(y,z)$ has the representation

$$u = \bar{u} + \sum_{j=1}^{\infty} u_j \psi_j(y,z), \quad \text{with} \quad u_j = \overline{u\psi_j}/(\overline{\psi_j^2})^{\frac{1}{2}}. \tag{5.1}$$

Thus, from the formula (3.2) for $\partial_\tau X_m$ and the solution (4.3) for f_{m0}, we find that the centroid displacement velocity for the mth mode ϕ_m is given by the series

$$\partial_\tau X_m = \sum_{l=1}^{\infty} \alpha_{ml} u_l \exp(-\lambda_l \tau). \tag{5.2}$$

The corresponding formula for $\partial_\tau D$ merely needs the replacement of α_{ml} by u_l (i.e. of $\phi_m(y,z)$ by $u(y,z)$):

$$\partial_\tau D = \sum_{l=1}^{\infty} u_l^2 \exp(-\lambda_l \tau) \tag{5.3}$$

(Smith 1981, equation (3.4)).

To choose the memory displacement velocity $v_m(\tau)$ for the mth mode non-uniformity, we ask: when is the two-term representation

$$\int_0^\infty f_{m0}(y,z,\tau)\, q_m\left(x - \int_0^\tau v_m(\tau')\,d\tau', t-\tau\right) d\tau + \int_0^\infty f_{m1}(y,z,\tau)\, \partial_x q_m\left(x - \int_0^\tau v_m(\tau')\,d\tau', t-\tau\right) d\tau, \tag{5.4}$$

as close as possible to the rudimentary one-term representation? Since f_{m0} decays exponentially fast from its initial value $\phi_m - \overline{\phi}_m$, the closest approximation is achieved if f_{m1} is orthogonal to this initial shape:

$$\overline{f_{m1}(\phi_m - \overline{\phi}_m)} = 0. \tag{5.5}$$

From the solution (4.6) for f_{m1}, we find that $v_m(\tau)$ is given by

$$\left.\begin{aligned} \partial_\tau E_m(\tau) \int_0^\tau [v_m(\tau') - \bar{u}]\,d\tau' &= \sum_{n=1}^{\infty} \alpha_{mn}^2 (u_{nn} - \bar{u})\, \tau \exp(-\lambda_n \tau) \\ &\quad + \sum_{n=1}^{\infty} \sum_{l \neq n} \alpha_{ml}\alpha_{mn} u_{ln} \left\{ \frac{\exp(-\lambda_n\tau) - \exp(-\lambda_l\tau)}{\lambda_l - \lambda_n} \right\}, \\ \text{with} \qquad \partial_\tau E_m(\tau) &= \sum_{l=1}^{\infty} \alpha_{ml}^2 \exp(-\lambda_l \tau). \end{aligned}\right\} \tag{5.6}$$

An aesthetically pleasing feature is that to obtain the formula for $v_0(\tau)$ we merely need replace α_{ml} by u_l (Smith 1981, equation (4.6)):

$$\partial_\tau D\int_0^\infty [v_0(\tau')-\bar{u}]\,d\tau' = \sum_{n=1}^{\infty} u_n^2(u_{nn}-\bar{u})\,\tau\exp(-\lambda_n\tau) + \sum_{n=1}^{\infty}\sum_{l\neq n} u_l u_n u_{ln}\left\{\frac{\exp(-\lambda_n\tau)-\exp(-\lambda_l\tau)}{\lambda_l-\lambda_n}\right\}. \tag{5.7}$$

In accord with physical intuition, at small times the memory velocity is a weighted average of the velocity profile:

$$v_m(0) = \overline{u(\phi_m-\bar{\phi}_m)^2}/\overline{(\phi_m-\bar{\phi}_m)^2}. \tag{5.8}$$

As time evolves the concentration distribution across the flow changes, and so does the memory velocity. An exceptional case is when the non-uniformity functions $\phi_m(y,z)$ coincide with the normal modes $\psi_m(y,z)$. In this case we have the neat result

$$v_m = u_{mm}. \tag{5.9}$$

6. Telegraph equation

For realistic flow geometries it is not practicable to compute more than just the first few eigenmodes $\psi_n(y,z)$. Thus, in practice the accuracy of the delay-diffusion equation (1.8) cannot be fully utilized. The most drastic simplification would be to include just a single eigenmode $\psi_1(y,z)$, and to truncate the series ((5.2), (5.3), (5.6), (5.9)) at the leading terms. This is equivalent to making a two-layer approximation to the flow, and leads to a telegraph equation (Thacker 1976).

Given the target of using a telegraph equation, it is natural to adjust the coefficients to achieve the best possible accuracy. Smith (1981) showed that for a uniform discharge the dispersion coefficient, the deficit variance, and the skewness are all asymptotically correct if we replace equations (5.3), (5.7) by the one-term approximations

$$\left.\begin{aligned} D(\tau) &= D(\infty)[1-\exp(-\mu\tau)], \quad D(\infty) = \overline{ug},\\ \mu &= \overline{ug}/\overline{g^2}, \quad v_0 = \overline{ug^2}/\overline{g^2}. \end{aligned}\right\} \tag{6.1}$$

Here the auxiliary function $g(y,z)$ satisfies the transverse diffusion equation

$$\left.\begin{aligned} \nabla.(\kappa\nabla g) &= \bar{u}-u, \quad \text{with} \quad \bar{g}=0;\\ \kappa\mathbf{n}.\nabla g &= 0 \quad \text{on } \partial A. \end{aligned}\right\} \tag{6.2}$$

With those approximations the delay-diffusion equation (1.8) for uniform discharges can be transformed to the telegraph equation

$$(\partial_t+v_0\partial_x+\mu)(\partial_t+\bar{u}\,\partial_x-\bar{\kappa}\,\partial_x^2)\,\bar{c}-\mu D(\infty)\,\partial_x^2\bar{c} = (\partial_t+v_0\partial_x+\mu)\,\bar{q}. \tag{6.3}$$

For completeness we record that the layer velocities u_+, u_- and the fractional areas a_+, a_-, occupied by the two layers are given by

$$\left.\begin{aligned} u_\pm &= \bar{u}+[\mu D(\infty)]^{\frac{1}{2}}\{s\pm[1+s^2]^{\frac{1}{2}}\}, \quad a_\pm = \tfrac{1}{2}\{1\mp s/[1+s^2]^{\frac{1}{2}}\},\\ \text{with} \quad s &= \tfrac{1}{2}(v_0-\bar{u})/[\mu D(\infty)]^{\frac{1}{2}}, \quad v_0 = u_++u_--\bar{u} \end{aligned}\right\} \tag{6.4}$$

(Smith 1981, equations (5.11)–(5.13)).

As throughout this paper, our concern is to determine the new right-hand-side terms needed to represent discharge non-uniformity. For a two-layer flow (Thacker 1976, equation (3)), the appropriate extra term is

$$-a_+a_-(u_+-u_-)\,\partial_x(q_+-q_-), \tag{6.5}$$

where q_+, q_- are the source strengths within the layers. Thus our modelling of non-uniformity merely entails the definition of q_+, q_-.

Aris (1956) showed that for a delta-function discharge

$$q = \delta(t)\,\delta(x)\,q(y,z) \tag{6.6}$$

the asymptotic centroid displacement caused by the non-uniformity is given by

$$\hat{X}(\infty) = \overline{gq}/\bar{q}. \tag{6.7}$$

This exact result is reproduced by the composite model equation (6.3), (6.4), provided that we define

$$q_+ = \bar{q}+\mu\overline{gq}/a_+(u_+-u_-), \quad q_- = \bar{q}-\mu\overline{gq}/a_-(u_+-u_-). \tag{6.8}$$

The resulting telegraph equation for non-uniform discharges can be written:

$$(\partial_t+v_0\partial_x+\mu)\,(\partial_t+\bar{u}\,\partial_x-\bar{\kappa}\,\partial_x^2)\,\bar{c}-\mu D(\infty)\,\partial_x^2\bar{c} = (\partial_t+v_0\partial_x+\mu)\,\bar{q}-\mu\,\partial_x(\overline{gq}). \tag{6.9}$$

By construction, the centroid and dispersion coefficient are asymptotically correct at large times after discharge. Moreover, as was noted by Chatwin (1970), the dominant contribution to the skewness at large times after discharge is independent of any source non-uniformity. Thus equation (6.9) inherits from the uniform discharge equation (6.3) the property that the skewness is asymptotically correct. Also, when there are two or more discharges with different non-uniformities, then the linearity of the expression $\overline{gq}$ ensures that the solutions for the bulk concentration distribution $\bar{c}(x,t)$ have the physically correct linear superposition property.

A bonus of using the telegraph-equation approximation is that, if the longitudinal diffusion $\bar{\kappa}$ can be neglected, then for a delta-function discharge (6.6) there is an explicit solution (Thacker 1976, equation (15)). We first introduce the dimensionless variables

$$\left.\begin{aligned} &X = [\mu/D(\infty)]^{\frac{1}{2}}(x-\bar{u}t), \quad T = \mu t, \quad U_\pm = s\pm[1+s^2]^{\frac{1}{2}},\\ &\xi = [\mu/D(\infty)]^{\frac{1}{2}}\,\overline{gq}/\bar{q} = (q_+-q_-)/2\bar{q}[1+s^2]^{\frac{1}{2}},\\ &C = c/\bar{q}[\mu/D(\infty)]^{\frac{1}{2}}. \end{aligned}\right\} \tag{6.10}$$

Between the extreme characteristics $U_-T < X < U_+T$ the solution can be expressed in terms of modified Bessel functions:

$$\left.\begin{aligned} C = &\left\{(1+s\xi)\,I_0(R)+\frac{[(1-\xi s+2s^2)\,T-(s-\xi)\,X]}{[T^2+2sXT-X^2]^{\frac{1}{2}}}\,I_0'(R)\right\}\exp\left(-\frac{[T+sX]}{2[1+s^2]}\right)\Big/4[1+s^2]^{\frac{3}{2}},\\ &\text{with} \qquad R = [T^2+2sXT-X^2]^{\frac{1}{2}}/2[1+s^2]. \end{aligned}\right\} \tag{6.11}$$

At the end points there are delta-function singularities

$$\left.\begin{aligned} C &= a_-(q_-/\bar{q})\,\delta(X-U_-T)\exp(-a_+T),\\ C &= a_+(q_+/\bar{q})\,\delta(X-U_+T)\exp(-a_-T). \end{aligned}\right\} \tag{6.12}$$

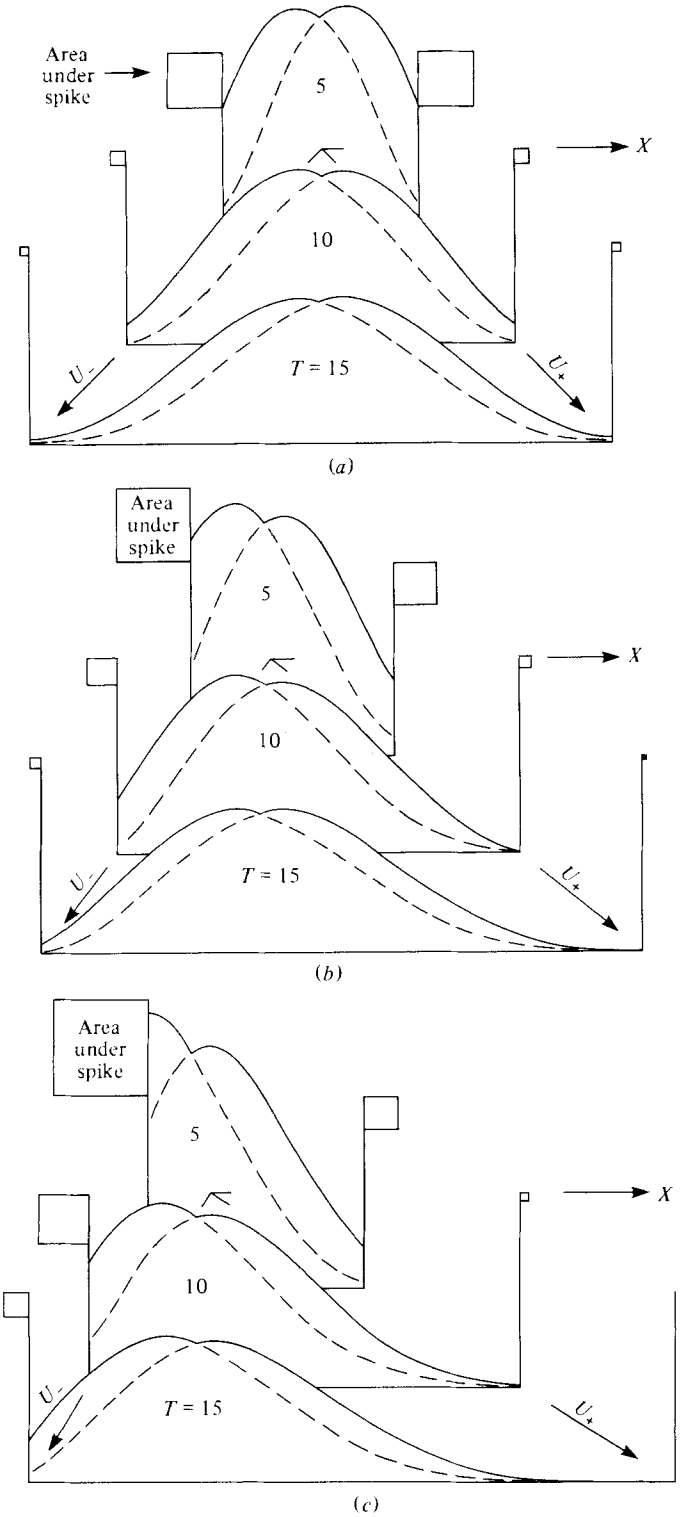

FIGURE 3. Concentration for a two-layer flow when the initial discharge is restricted to just one of the layers. The lower of the two concentrations at each point is indicated by the dashed lines.

The inclusion of longitudinal diffusion removes these spikes (Thacker 1976, § 3), but the advantage of an explicit solution is then lost.

For a positive discharge in a two-layer flow, the parameter ξ measuring the source non-uniformity is restricted to the range

$$-2a_+ \leqslant \xi \leqslant 2a_-. \tag{6.13}$$

The extremes correspond to discharges in just one of the layers. Figures (3*a–c*) compare these extreme cases, when the skewness parameter has the values $s = 0, \frac{1}{4}, \frac{1}{2}$. The left-hand spike and the higher concentrations (continuous line) towards the rear are associated with the discharge in the slow-moving layer, while the right-hand spike and the higher concentrations towards the front are associated with a discharge in the fast-moving layer. For negative s the profiles are mirror images about $X = 0$. Although the centroids rapidly reach their asymptotic positions, the influence of the discharge conditions upon the overall shape persists to remarkably large times. The e-folding time for the free decay of concentration variations across the flow corresponds to a non-dimensional time $T = 1$. It is the continual regeneration of concentration variations in regions of high concentration gradient which prolongs the influence of the initial conditions. We recall that the pronounced skewness arises from the fact that the advection velocity $v_0 = u_+ + u_- - \bar{u}$ for the concentration variations (i.e. for the memory effects) can differ from the bulk velocity $\bar{u}$ (Smith 1981, equation (4.9)).

7. An off-centre discharge in pipe flow

We now illustrate the application of the above analysis to the dispersion of a solute discharged from a narrow-bore syringe in laminar pipe flow. The weighted averages

$$\overline{(\bar{u}-u)\,l_1}, \quad \overline{(\bar{u}-u)f_{m0}}$$

in the longitudinal dispersion equation (3.1) mean that the angular dependence of the concentration distribution is not important. Thus we can regard the discharge as being spread around an annulus. In the limit of small discharge area, we take the fundamental equations (2.1) to have the form

$$\left.\begin{aligned} &\partial_t c + 2\bar{u}(1-(r/a)^2)\,\partial_x c - \kappa\partial_x^2 c - \frac{\kappa}{r}\frac{\partial}{\partial r}\left(r\frac{\partial c}{\partial r}\right) = \frac{a^2}{2b}\,\delta(r-b)\,\bar{q}(x,t), \\ &\text{with} \qquad \partial c/\partial r = 0 \quad \text{on} \quad r = a. \end{aligned}\right\} \tag{7.1}$$

Here a is the pipe radius, b the discharge position, κ the constant diffusivity, and r the radial co-ordinate. We note that because of the assumed circular symmetry the cross-sectional average values can be written

$$\bar{c} = \frac{2}{a^2}\int_0^a c(x,r,t)\,r\,dr. \tag{7.2}$$

The appropriate eigenfunctions for the analysis of the transverse dispersion are Bessel function of order zero:

$$\left.\begin{aligned} &\phi_n = \psi_n/(\overline{\psi_n^2})^{\frac{1}{2}} = J_0(\gamma_n(r/a))/J_0(\gamma_n), \\ &\text{with} \qquad J_0'(\gamma_n) = 0, \quad \lambda_n = \gamma_n^2\kappa/a^2. \end{aligned}\right\} \tag{7.3}$$

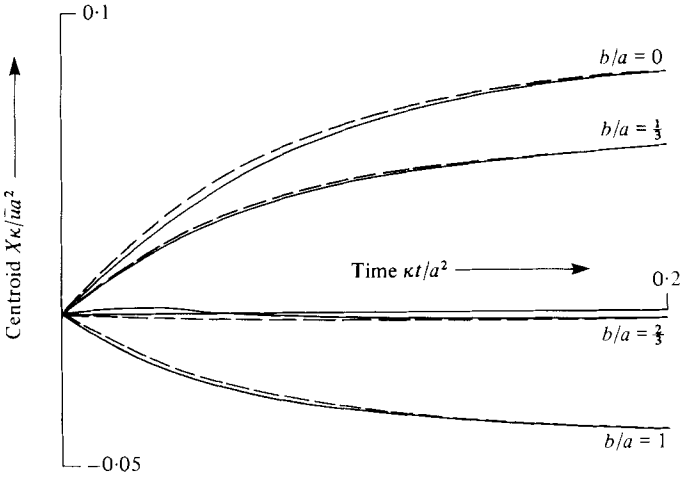

FIGURE 4. Centroid displacement for different discharge positions in Poiseuille pipe flow.

The coefficients q_m, u_m in the eigenfunction expansions for the source distribution (2.2) and for the velocity profile (5.1) are given by

$$\left.\begin{aligned} q_m &= J_0(\gamma_m(b/a))/J_0(\gamma_m), \\ u_m &= -8\bar{u}/\gamma_m^2. \end{aligned}\right\} \tag{7.4}$$

In the double sequence (4.4) the diagonal and the off-diagonal elements are given by

$$u_{mm} = \tfrac{4}{3}\bar{u}, \quad u_{mn} = -8\bar{u}(\gamma_m^2+\gamma_n^2)/(\gamma_m^2-\gamma_n^2)^2. \tag{7.5}$$

From (5.2) it follows that the total centroid displacement, summed over all the modes, is given by

$$\hat{X} = -\frac{8\bar{u}a^2}{\kappa}\sum_{m=1}^{\infty}[J_0(\gamma_m(b/a))/\gamma_m^4 J_0(\gamma_m)][1-\exp(-\gamma_m^2\kappa\tau/a^2)]. \tag{7.6}$$

Figure 4 shows the time dependence of $\hat{X}$ for several different source positions. For other discharge distributions across the flow, the centroid displacement is the appropriate weighted average of the point-discharge results. A noteworthy feature is that the displacement is not necessarily monotonic. Dewey & Sullivan (1982) explain this feature in terms of the initial tendency for the contaminant to be preferentially diffused away from the impermeable boundary and hence into the faster-moving fluid.

Aris (1956, equation (24), (32)) observed that at large times after discharge the centroid displacement $\hat{X}(\infty; b)$ for a point discharge at b is identical with the centroid displacement $X(b; \infty)$ as a function of position across the flow for a uniform discharge. This reciprocal relationship between point and uniform discharges can be shown to be valid for all times. Thus the exact results shown in figure 4 are identical with those presented by Smith (1982, figure 1*a*) for the dual problem.

To apply the telegraph-equation approximation we first calculate the auxiliary function $g(r)$:

$$g(r) = \frac{\bar{u}a^2}{24\kappa}\left\{2-6\left(\frac{r}{a}\right)^2+3\left(\frac{r}{a}\right)^4\right\}. \tag{7.7}$$

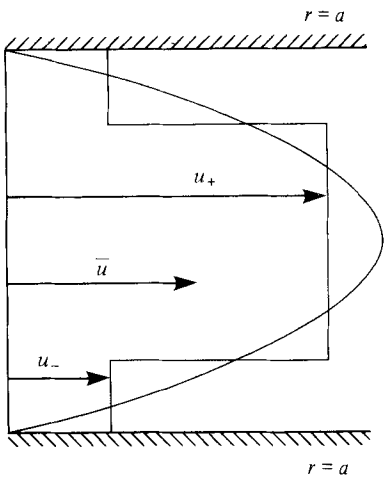

FIGURE 5. Two-layer approximation to the velocity profile for Poiseuille pipe flow.

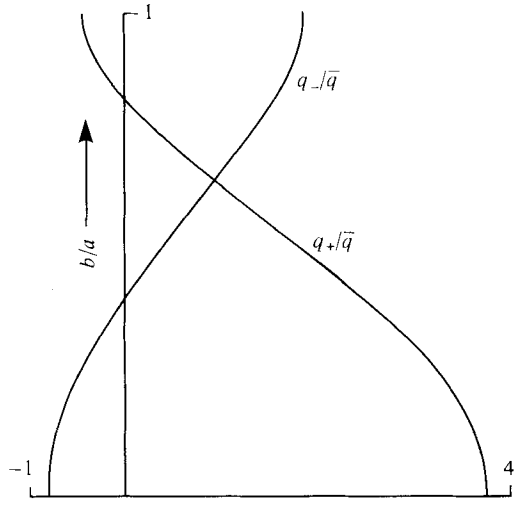

FIGURE 6. Two-layer decomposition of the source strength as a function of the discharge position across Poiseuille pipe flow.

Using this formula in (6.1), (6.4), we obtain the results

$$\left.\begin{aligned} D(\infty) &= \bar{u}^2a^2/48\kappa, \quad \mu = 15\kappa/a^2, \quad v_0-\bar{u} = \tfrac{1}{4}\bar{u}, \\ s &= \sqrt{\tfrac{1}{20}} = 0{\cdot}2236, \quad a_+ = \tfrac{1}{2}(1-\sqrt{\tfrac{1}{21}}) = 0{\cdot}3909, \\ a_- &= \tfrac{1}{2}(1+\sqrt{\tfrac{1}{21}}) = 0{\cdot}6091, \quad u_+ = \tfrac{1}{8}(9+\sqrt{21})\,\bar{u} = 1{\cdot}698\bar{u}, \\ u_- &= \tfrac{1}{8}(9-\sqrt{21})\,\bar{u} = 0{\cdot}5522\,\bar{u}. \end{aligned}\right\} \tag{7.8}$$

Figure 5 shows the two-layer approximation to the velocity profile, and figure 6 shows the decomposition (6.8) for the source distribution. The dashed curves in figure 4 show the two-layer approximation to the centroid displacement

$$\hat{X} = g(b)\,[1-\exp(-\mu\tau)]. \tag{7.9}$$

Although the approximation fails to exhibit the non-monotonicity, the overall error is reasonably small.

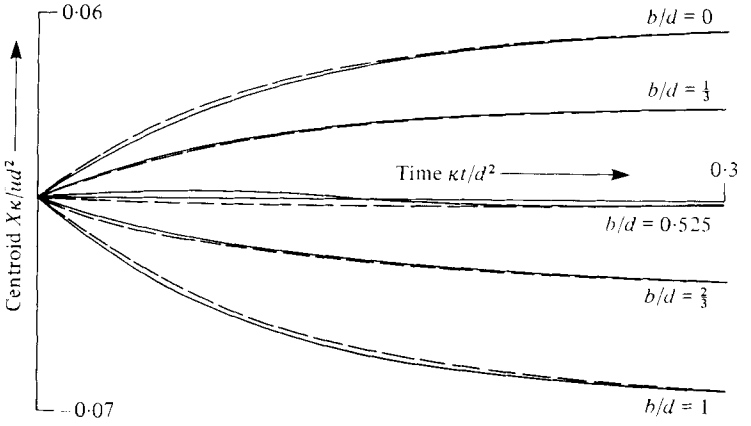

FIGURE 7. Centroid displacement for different discharge positions in plane Poiseuille flow.

8. Plane Poiseuille flow

As a second illustrative example, we follow Smith (1981, § 8), and consider a point discharge in plane Poiseuille flow:

$$u(y) = \tfrac{3}{2}\bar{u}[1-(y/d)^2], \quad q = \delta(y-b)\,\bar{q}(x,t) \quad (-d < y < d). \tag{8.1}$$

The relevant eigenmodes and coefficients are

$$\left.\begin{aligned} \phi_m &= \psi_m/(\overline{\psi_m^2})^{\frac{1}{2}} = \sqrt{2}\cos(m\pi y/d), \quad \lambda_m = m^2\pi^2\kappa/d^2, \\ q_m &= \sqrt{2}\cos(m\pi b/d), \quad u_m = (-1)^{m+1}3\sqrt{2}\,\bar{u}/m^2\pi^2, \\ u_{mm} - \bar{u} &= \frac{-3\bar{u}}{4m^2\pi^2}, \quad u_{mn} = \frac{6(m^2+n^2)}{(m^2-n^2)^2}\frac{(-1)^{m+n+1}}{\pi^2}\bar{u}. \end{aligned}\right\} \tag{8.2}$$

The centroid displacement, summed over all the modes, is given by

$$\hat{X} = \frac{6\bar{u}d^2}{\pi^4\kappa}\sum_{m=1}^{\infty}\frac{(-1)^{m+1}}{m^4}\cos\left(\frac{m\pi b}{d}\right)\left[1-\exp\left(-\frac{m^2\pi^2\kappa t}{d^2}\right)\right] \tag{8.3}$$

(see figure 7). Again, there is non-monotonicity near $u(y) = \bar{u}$ (i.e. near $b = d/\sqrt{3}$), and duality with the uniform discharge problem (Smith 1982, figure 4*a*).

The auxiliary function $g(y)$ required for the telegraph-equation approximation is given by

$$g(y) = \frac{\bar{u}d^2}{120\kappa}\left\{7 - 30\left(\frac{y}{d}\right)^2 + 15\left(\frac{y}{d}\right)^4\right\}. \tag{8.4}$$

From (6.1), (6.4), this leads to the two-layer approximations

$$\left.\begin{aligned} D(\infty) &= 2\bar{u}^2d^2/105\kappa, \quad \mu = 10\kappa/d^2, \quad v_0 - \bar{u} = -\tfrac{4}{33}\bar{u}, \\ s &= -\tfrac{1}{33}\sqrt{21} = 0{\cdot}1389, \quad a_+ = 0{\cdot}5688, \quad a_- = 0{\cdot}4312, \\ u_+ &= 1{\cdot}380\bar{u}, \quad u_- = 0{\cdot}4988\bar{u}. \end{aligned}\right\} \tag{8.5}$$

The dashed curves in figure 7 show that the monotonic approximation (7.9) to the centroid displacement is generally quite accurate.

Figure 8 shows the two-layer approximation to the velocity profile. At first sight

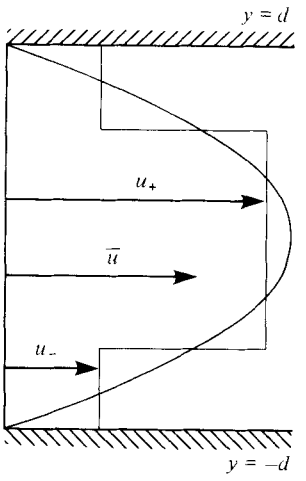

FIGURE 8. Two-layer approximation to the velocity profile for plane Poiseuille flow.

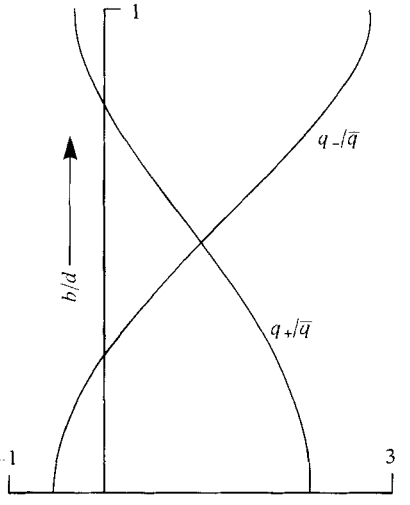

FIGURE 9. Two-layer decomposition of the source strength as a function of discharge position across plane Poiseuille flow.

there would seem to be a close resemblance to the pipe-flow velocity decomposition as shown in figure 5. However, the difference between Cartesian and cylindrical co-ordinates gives extra weight to the faster-moving central region. Thus, unlike the pipe-flow situation, the greater part of the fluid is moving faster than $\bar{u}$. This means that the tail of the concentration distribution is associated with the slower-moving fluid, and hence that the skewness is negative (as can be seen in figure 2).

Figure 9 shows the splitting (6.8) between the two layers of the source strength. As we should expect, when the discharge is positioned in the faster-moving parts of the flow, greater weight is given to the discharge strength q_+ in the fast layer. Within about $0{\cdot}3d$ of the centre of the flow, the forward centroid displacement is so great that q_- becomes negative. This has the consequence that far to the rear of the concentration distribution there will be spurious negative concentrations. Similarly, for discharges

within about $0{\cdot}2d$ of the walls, there will be small negative concentrations far forward of the main concentration distribution.

9. Open-channel flow

Continuing as in Smith (1981), we consider a point discharge in a logarithmic velocity profile

$$\left.\begin{aligned} u &= \bar{u} + (u_*/k)\,(1+\ln(1+z/h)), \quad \kappa = ku_*h(1+z/h)(-z/h), \\ q &= \delta(z-b)\,\bar{q}(x,t) \end{aligned}\right\} \quad (-h < z < 0), \tag{9.1}$$

where k is the Kármán constant. The eigenmodes and coefficients are

$$\left.\begin{aligned} \phi_m &= \psi_m/(\overline{\psi_m^2})^{\frac{1}{2}} = (2m+1)^{\frac{1}{2}} P_m(2(z/h)+1), \\ \lambda_m &= m(m+1)\,ku_*/h, \quad q_m = (2m+1)^{\frac{1}{2}} P_m(2(b/h)+1), \\ u_m &= (2m+1)^{\frac{1}{2}}(-1)^{m+1} u_*/km(m+1), \\ u_{mm} - \bar{u} &= -\frac{u_*}{k}\left[-\frac{2m}{2m+1} + 2\sum_{j=1}^{2m}\frac{(-1)^{j-1}}{j}\right], \\ u_{mn} &= \frac{u_*}{k}\frac{(2m+1)^{\frac{1}{2}}(2n+1)^{\frac{1}{2}}(-1)^{m-n+1}}{|n-m|\,(m+n+1)}, \end{aligned}\right\} \tag{9.2}$$

where P_m denotes the Legendre polynomial of degree m. The centroid displacement, summed over all the modes, is given by

$$\hat{X} = \frac{h}{k^2}\sum_{m=1}^{\infty}\frac{(2m+1)(-1)^{m+1}}{m^2(m+1)^2} P_m(2(b/h)+1)\,[1-\exp(-m(m+1)\,ku_*t/h)]. \tag{9.3}$$

This is shown in figure 10 with the Kármán constant chosen to be $k = 0{\cdot}4$.

It deserves comment that, although the velocity becomes singular and the diffusivity tends to zero at the channel bed, the centroid displacement remains finite. If we average out the longitudinal concentration variations, then near the channel bed the vertical structure of the concentration distribution satisfies the equation

$$\partial_t c^{(0)} = \partial_z(ku_*(h+z)\,\partial_z c^{(0)}). \tag{9.4}$$

For a unit point discharge at $z = -h$, the local solution is

$$c^{(0)} = \exp(-(h+z)/ku_*t)/ku_*t, \tag{9.5}$$

and expands linearly with time. The corresponding longitudinal displacement velocity involves a weighted average with respect to the velocity profile

$$\begin{aligned} d\hat{X}/dt &= \int_{-h}^{0}(u(z)-\bar{u})\,c^{(0)}\,dz \doteq \int_{-h}^{\infty}(u(z)-\bar{u})\,c^{(0)}\,dz \\ &= \frac{u_*}{k}\left[1+\int_0^{\infty}\exp(-\eta)\ln\eta\,d\eta + \ln(ku_*t/h)\right]. \end{aligned} \tag{9.6}$$

Thus for small times there is a logarithmic singularity in the centroid displacement velocity. However, this is an integrable singularity and the total displacement remains bounded.

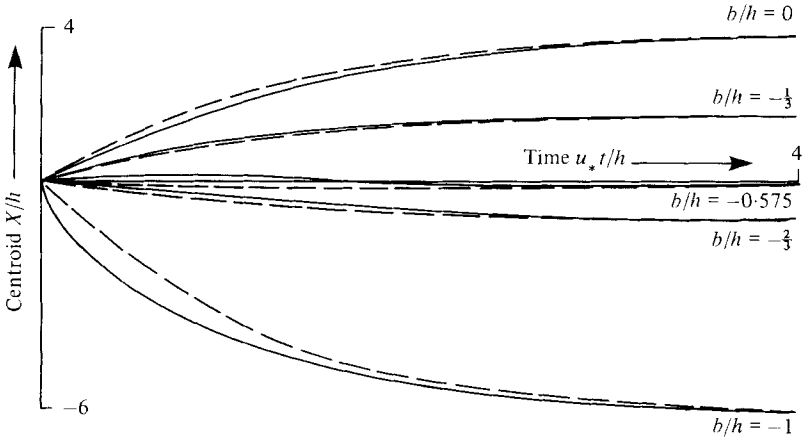

FIGURE 10. Centroid displacement for different discharge depths in turbulent open-channel flows.

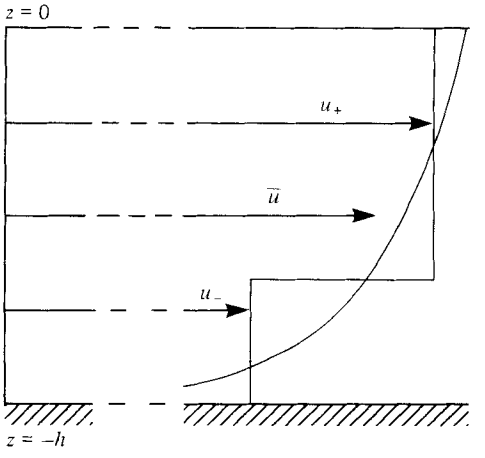

FIGURE 11. Two-layer approximation to the velocity profile for turbulent open-channel flow.

Unfortunately, for the telegraph-equation approximation it is not possible to express the auxiliary function $g(z)$ in closed form:

$$g(z) = \frac{h}{k^2}\left\{1 - \int_{-h}^{z} \frac{\ln(1+z/h)\,dz}{z}\right\}$$

$$= \frac{h}{k^2}\sum_{m=1}^{\infty}(-1)^{m+1}(2m+1)\,P_m(2(z/h)+1)/m^2(m+1)^2. \tag{9.7}$$

Thus the integrals (6.1) have to be evaluated numerically (Smith 1981, equation (9.12)):

$$D(\infty) = \frac{0{\cdot}4041hu_*}{k^3}, \quad \mu = \frac{2{\cdot}107ku_*}{h}, \quad v_0 - \bar{u} = -\frac{0{\cdot}6781u_*}{k}. \tag{9.8}$$

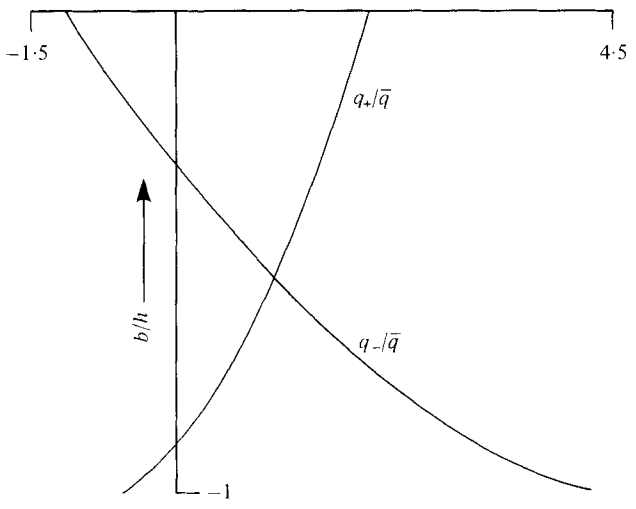

FIGURE 12. Two-layer decomposition of the source strength as a function of discharge depth in turbulent open-channel flow.

The two-layer specification (6.4) is then

$$\left.\begin{aligned} s &= -0{\cdot}3674, \quad a_+ = 0{\cdot}6724, \quad a_- = 0{\cdot}3276, \\ u_+ &= \bar{u} + 0{\cdot}644 u_*/k, \quad u_- = \bar{u} - 1{\cdot}322 u_*/k \end{aligned}\right\} \tag{9.9}$$

(see figures 11, 12). The velocity shear is much more pronounced than in the previous two examples. This has the consequences that there is a stronger dependence of q_+, q_- upon discharge position, and that the two-layer approximation to $\hat{X}(t)$ is of reduced usefulness. The most extreme example is when the discharge is at the channel bed. Near $t = 0$, the two-layer formula (7.9) fails to reproduce the singularity in $\partial_t \hat{X}$.

10. Concluding remarks

The differing statuses of the three alternative model equations

$$\partial_t \bar{c} + [\bar{u} + \partial_t \hat{X}]\,\partial_x \bar{c} - [\bar{\kappa} + D(t) + \hat{D}(t) - \hat{X}\,\partial_t \hat{X}]\,\partial_x^2 \bar{c} = 0, \tag{10.1}$$

$$\partial_t \bar{c} + \bar{u}\,\partial_x \bar{c} - \bar{\kappa}\,\partial_x^2 \bar{c} - \int_0^\infty \partial_\tau D\,\partial_x^2 \bar{c}\left(x - \int_0^\tau v_0(\tau')\,d\tau', t - \tau\right) d\tau$$

$$= \bar{q} - \sum_{m=1}^{\infty} \int_0^\infty \partial_\tau X_m\,\partial_x q_m\left(x - \int_0^\tau v_m(\tau')\,d\tau', t - \tau\right) d\tau, \tag{10.2}$$

$$(\partial_t + v_0\partial_x + \mu)(\partial_t + \bar{u}\,\partial_x - \bar{\kappa}\,\partial_x^2)\,\bar{c} - \mu D(\infty)\,\partial_x^2 \bar{c} = (\partial_t + v_0\partial_x + \mu)\,\bar{q} - \mu\,\partial_x(\overline{gq}) \tag{10.3}$$

deserve emphasis. Gill & Sankarasubramanian (1971) derived the diffusion approximation (10.1) from the full three-dimensional advection–diffusion equation (2.1). Unfortunately, truncation at any level of their infinite-order differential equation (9) necessarily violates the linear superposition property. The delay-diffusion equation (10.2) is likewise derived from the full equations, and is also the truncation of an infinite-order equation (3.1). However, the linear superposition property is preserved

at all levels. Finally, the telegraph equation (10.3) is an *ad hoc* approximation which is easy to use and is physically sound by virtue of its connection with two-layer flows (Thacker 1976).

I wish to thank The Royal Society and British Petroleum for financial support.

REFERENCES

ARIS, R. 1956 On the dispersion of a solute in a fluid flowing through a tube. *Proc. R. Soc. Lond.* A **235**, 67–77.

CHATWIN, P. C. 1970 The approach to normality of the concentration distribution of a solute in solvent flowing along a pipe. *J. Fluid Mech.* **43**, 321–352.

DEWEY, R. J. & SULLIVAN, P. J. 1982 Longitudinal diffusion at small times. *J. Fluid Mech.* (submitted).

GILL, W. N. & SANKARASUBRAMANIAN, R. 1970 Exact analysis of unsteady convective diffusion. *Proc. R. Soc. Lond.* A **316**, 341–350.

GILL, W. N. & SANKARASUBRAMANIAN, R. 1971 Dispersion of a non-uniform slug in time-dependent flow. *Proc. R. Soc. Lond.* A **322**, 101–117.

KRISHNAMURTHY, S. & SUBRAMANIAN, R. S. 1977 Exact analysis of field-flow fractionation. *Sep. Sci. Tech.* **12**, 347–379.

JAYARAJ, K. & SUBRAMANIAN, R. S. 1978 On relaxation phenomena in field-flow fractionation. *Sep. Sci. Tech.* **13**, 791–871.

MARON, V. I. 1978 Longitudinal diffusion in a flow through a tube. *Int. J. Multiphase Flow* **4**, 339–355.

SMITH, R. 1981 A delay-diffusion description for contaminant dispersion. *J. Fluid Mech.* **105**, 469–486.

SMITH, R. 1982 Gaussian approximation for contaminant dispersion. *Quart. J. Mech. Appl. Math.* (to appear).

TAYLOR, G. I. 1953 Dispersion of soluble matter in solvent flowing slowly through a tube. *Proc. R. Soc. Lond.* A **219**, 186–203.

TAYLOR, G. I. 1959 The present position in the theory of turbulent diffusion. *Adv. Geophys.* **6**, 101–111.

THACKER, W. C. 1976 A solvable model of shear dispersion. *J. Phys. Oceanogr.* **6**, 66–75.